Development 138, 4721-4732 (2011) doi:10.1242/dev.064998

Vascular endothelial and endocardial progenitors differentiate as cardiomyocytes in the absence of Etsrp/Etv2 function

Sharina Palencia-Desai[1,2], Vikram Kohli[1], Jione Kang[3], Neil C. Chi[4], Brian L. Black[3] and Saulius Sumanas[1,2,*]

SUMMARY

Previous studies have suggested that embryonic vascular endothelial, endocardial and myocardial lineages originate from multipotential cardiovascular progenitors. However, their existence in vivo has been debated and molecular mechanisms that regulate specification of different cardiovascular lineages are poorly understood. An ETS domain transcription factor Etv2/Etsrp/ER71 has been recently established as a crucial regulator of vascular endothelial differentiation in zebrafish and mouse embryos. In this study, we show that *etsrp*-expressing vascular endothelial/endocardial progenitors differentiate as cardiomyocytes in the absence of Etsrp function during zebrafish embryonic development. Expression of multiple endocardial specific markers is absent or greatly reduced in Etsrp knockdown or mutant embryos. We show that Etsrp regulates endocardial differentiation by directly inducing endocardial *nfatc1* expression. In addition, Etsrp function is required to inhibit myocardial differentiation. In the absence of Etsrp function, *etsrp*-expressing endothelial and endocardial progenitors initiate myocardial marker *hand2* and *cmlc2* expression. Furthermore, Foxc1a function and interaction between Foxc1a and Etsrp is required to initiate endocardial development, but is dispensable for the inhibition of myocardial differentiation. These results argue that Etsrp initiates endothelial and endocardial, and inhibits myocardial, differentiation by two distinct mechanisms. Our findings are important for the understanding of genetic pathways that control cardiovascular differentiation during normal vertebrate development and will also greatly contribute to the stem cell research aimed at regenerating heart tissues.

KEY WORDS: Endocardial, Endothelial, Multipotent progenitor, Myocardial, Zebrafish

INTRODUCTION

The heart is composed of diverse muscle and non-muscle cell lineages. Until recently, it has been believed that cardiac progenitor cells commit early during development to exclusively generate cardiomyocytes, whereas other heart lineages such as endocardial cells are specified independently. However, a growing body of evidence from multiple laboratories suggest that, with respect to lineage diversification, there may be a single stem/progenitor cell that can generate all major cell types during heart formation (Kattman et al., 2006; Moretti et al., 2006; Wu et al., 2006; Yang et al., 2008). However, signaling pathways that direct the formation of these cell lineages remain to be elucidated.

Although it is difficult to study cardiovascular lineage formation in mammals due to embryo inaccessibility, the zebrafish offers an advantageous in vivo system to dissect the mechanisms of cardiovascular lineage formation. Similar to mammalian embryos, zebrafish endocardial, myocardial and vascular endothelial cells form in close vicinity within the anterior lateral plate mesoderm (ALPM). Lineage-tracing experiments in avian and zebrafish embryos have shown that the spatial separation of endocardial and myocardial progenitors happens very early and can already be observed in early gastrula stage embryos (Lee et al., 1994; Keegan et al., 2004). However, cardiac progenitor cells retain flexibility to adopt a different cardiovascular fate and do not commit to their final cell fates until later somitogenesis stages. The zebrafish ALPM region rostral to the myocardium-forming region harbors latent myocardial developmental potential (Schoenebeck et al., 2007). This rostral ALPM region normally gives rise to head vessels, myeloid cells and endocardium. Expression of the transcription factor *hand2* corresponds to the myocardium forming region, as demonstrated by fate-mapping studies (Schoenebeck et al., 2007). In *cloche* (*clo*) mutants, which are almost completely devoid of endothelial, endocardial and hematopoietic cells (Stainier et al., 1995; Liao et al., 1997; Liao et al., 1998), *hand2* expression extends beyond its normal boundary, exhibiting strong expression throughout the rostral ALPM, resulting in a significant increase in cardiomyocytes (Schoenebeck et al., 2007). Similarly, double knockdown of *etsrp* and *scl*, two known regulators of vasculogenesis and hematopoiesis, respectively, resulted in a similar rostral expansion of myocardial *hand2* expression. Conversely, combinatorial overexpression of *scl* and *etsrp* RNA resulted in the reduction of myocardial-specific *hand2* and *cmlc2* (*myl7* – Zebrafish Information Network) expression. Similar expansion of hematovascular and loss of myocardial development was recently observed upon inhibition of FGF signaling (Simoes et al., 2011). However, it is unclear whether the observed myocardial expansion in the absence of hematovascular development is due to the cell fate switch of hematovascular progenitors into myocardial progenitors. Furthermore, the molecular mechanism of the suppression of myocardial differentiation in the rostral ALPM region during normal development is not understood.

[1]Division of Developmental Biology, Cincinnati Children's Hospital Medical Center, Cincinnati, OH 45229, USA. [2]University Of Cincinnati College of Medicine, Cincinnati, OH 45229, USA. [3]Department of Biochemistry and Biophysics, University of California, San Francisco, CA 94158 USA. [4]Department of Medicine, Division of Cardiology, University of California, San Diego School of Medicine, San Diego, CA 92093, USA.

*Author for correspondence (saulius.sumanas@cchmc.org)

Accepted 6 September 2011

Although significant progress has been made towards elucidating the morphogenetic events and transcriptional control underlying the patterning of myocardium, the early endocardial development remains still poorly understood (Lough and Sugi, 2000; Harris and Black, 2010). Similar to mammalian embryos, endocardial cells in zebrafish originate bilaterally within the anterior lateral plate mesoderm (ALPM). Vascular endothelial and endocardial cells share expression of multiple markers, including *cdh5*, *fli1* and *kdrl* (Brown et al., 2000; Larson et al., 2004; Sumanas et al., 2005). Very few molecular markers are specific to endocardium; one of them is Nfatc1, which is expressed in the mouse endocardial, but not vascular endothelial, cells, indicating that the two endothelial subtypes are biochemically distinct (de la Pompa et al., 1998). Although Nfatc1 homologs have not been previously characterized in zebrafish, *fibronectin 1* (*fn1*) expression is thought to label early endocardial but not vascular endothelial precursors (Trinh and Stainier, 2004). In vitro studies have demonstrated that endocardial lineage can develop from the same multipotent progenitor cells as myocardial and vascular endothelial lineages (Misfeldt et al., 2009). Endocardial precursors can be distinguished from other vascular endothelial cells as they migrate medially and posteriorly, and fuse at the midline between the 15- and 18-somite stages (Bussmann et al., 2007). Subsequently, they undergo a complex leftward movement to position the endocardial primordium at the left side of the embryo where they form the lining of the primitive heart tube. However, the signaling pathways that regulate specification, migration and differentiation of endocardial progenitors in vivo are largely unknown.

Previous studies have established that an ETS domain transcription factor, Etsrp/Etv2 functions on top of the transcriptional cascade that regulates vascular endothelial development in zebrafish (Sumanas and Lin, 2006; Pham et al., 2007). Morpholino knockdown of Etsrp function results in nearly complete loss of early vascular development as angioblasts fail to differentiate or migrate towards the midline. Etsrp overexpression alone is sufficient to induce precocious and ectopic expression of multiple vascular-specific markers, including *kdrl*, *fli1* and *cdh5* (Sumanas and Lin, 2006; Pham et al., 2007). Etsrp function is conserved during vertebrate development, with mouse ER71/Etv2 and human ETV2 proteins representing functional orthologs of Etsrp (Lee et al., 2008; Sumanas et al., 2008). Homozygous *Etv2* knockout mouse embryos display the lack of blood islands, as well as endothelial and endocardial lineages, and die before E11.0 (Lee et al., 2008; Ferdous et al., 2009). It has been shown that multiple vascular endothelial specific genes share a conserved regulatory enhancer that cooperatively binds Etsrp/Etv2 and FoxC family of transcription factors (De Val et al., 2008). However, only limited analysis of cardiac defects has been performed in mouse *Etv2* knockout embryos and its role in the formation of endocardial and myocardial lineages is poorly understood.

In this study, we have investigated the requirement of Etsrp for the development of endocardial and myocardial lineages in the zebrafish model system. We show that, in the absence of Etsrp function, early endocardial progenitors fail to differentiate, whereas myocardial progenitors expand into the rostral ALPM region. Furthermore, *etsrp*-expressing (*etv2* – Zebrafish Information Network) endocardial progenitors initiate myocardial marker expression and differentiate as cardiomyocytes in the absence of Etsrp function. We further show that Foxc1a function is required for early endocardial differentiation but is dispensable for the inhibition of myocardial differentiation within the rostral ALPM. These results argue that Etsrp/Etv2 acts as a crucial switch in cardiovascular lineage differentiation, and it promotes endocardial and inhibits myocardial differentiation via two different mechanisms.

MATERIALS AND METHODS

Zebrafish lines

The following zebrafish lines were used for experiments: Tg(*kdrl*:EGFP)^{s843} (Jin et al., 2005), Tg(*fli1*:EGFP)^{y1} (Lawson and Weinstein, 2002); Tg (cmlc2:GFP)^{twu34} (Huang et al., 2003); etsrp^{y11} (Pham et al., 2007), Tg(*etsrp*:EGFP)^{ci1} (Proulx et al., 2010) and wild type (Ekkwill). A *cmlc2:*mCherry construct was generated by cloning a 900 bp fragment of the *cmlc2* promoter (Huang et al., 2003) upstream of a promoter-less mCherry construct (Shaner et al., 2004). Five *Tg(cmlc2:*mCherry*)* founders were recovered with nearly identical expression patterns and levels. *Tg(cmlc2:*mCherry*)^{sd7}* exhibited the strongest expression and thus was employed for these studies.

Embryos were incubated at 28.5°C for analysis at 24 hpf and later stages, and at 23.5°C for analysis during somitogenesis stages. Embryos were staged as described previously (Kimmel et al., 1995). Embryos were treated with 1-pheny-2-thiourea (PTU) to inhibit pigment formation for stages 24 hpf and beyond. *etsrp$^{y11-/-}$* mutants were identified prior to 24 hpf by downregulation of *fli1*:GFP expression or at 24 hpf by the absence of intersomitic vessels and defective development of the axial vessels prior to in situ hybridization as previously reported (Pham et al., 2007).

Microinjection of MOs

For the majority of Etsrp knockdown experiments, 12.5 ng total of *etsrp* MO1 and MO2 1:1 mixture was injected at the 1- to 2-cell stage (Sumanas and Lin, 2006). To knock down *etsrp* function in Tg(*etsrp*:GFP)^{ci1} line, 20 ng MO1 was used because MO2 is designed against the 5′UTR region and inhibits *etsrp*:GFP fluorescence. MO1 injection phenocopied the *etsrp^{y11}* mutant phenotype and no other morphological abnormalities were observed. In the majority of the experiments, a single *Foxc1*a MO2 (sequence CGCCTGCATGACTGCTCTCCAAAAC) was injected at doses 1.5-3.0 ng per embryo, as reported previously (De Val et al., 2008). For 4 ng injections, a mixture of 4 ng of *foxc1a* MO2 and 2.5 ng *p53* MO was injected to alleviate non-specific effects associated with high MO doses (Robu et al., 2007). For *foxc1a* MO cocktail injections, shown in Fig. S5 in the supplementary material, a mixture of 3 ng *foxc1a* MO1 (Topczewska et al., 2001), 3 ng *foxc1a* MO2 and 3.75 ng p53 MO was injected.

In situ hybridization

In situ hybridization was performed as previously described (Jowett, 1999). A two-color in situ hybridization protocol was used as described (Sumanas et al., 2008). To synthesize DIG-labeled probes, *nfatc1* (Open Biosystems, catalog number EDR1052-9118306, Accession Number CN320837) and *fn1* (Open Biosystems, catalog number EDR1052-96834665) cDNA clones, both in pExpress1 vector, were digested with *Eco*RI and transcribed with T7 RNA polymerase (Promega). *flk1/kdrl* (Thompson et al., 1998), *cdh5* (Sumanas et al., 2005); *hand2* (Yelon et al., 2000) and *cmlc2* (Yelon et al., 1999) probes were synthesized as described. *cmlc2* expression area was quantified by measuring width and length of the staining area using Adobe Photoshop CS2 in wild-type and Etsrp morphant embryos.

Immunofluorescent detection of etsrp:GFP

To perform double staining of *fn1* and *etsrp*:GFP, immediately following in situ hybridization, embryos were washed in PBST, manually deyolked and blocked for 1 hour at room temperature in saponin blocking solution (SBS) [0.2% (w/v) saponin, 2 mg/ml BSA, 10% sheep serum (v/v), 1×PBS]. Embryos incubated in anti-GFP-Alexa488 (Invitrogen #A21311) at 4 μg/ml diluted in SBS overnight at 4°C. Embryos were washed three times for 10 minutes per wash with PBS/0.2% saponin and incubated with goat anti rabbit-Alexa488 (Invitrogen #A11078) at 4 μg/ml diluted in SBS for 2 hours at room temperature. After washing with PBS/0.2% saponin, PBS and 30% glycerol/PBS, embryos were ventrally flat mounted in Vectashield (Vector Labs H-1000).

Cell transplantation

Donor *cmlc2*:GFP embryos were injected with a mixture of *etsrp* DNA (55 pg) and tetramethyl rhodamine isothiocyanate (TRITC)-dextran (2 ng; Mw 2 MDa; Sigma-Aldrich) into the blastomere at the one-cell stage. Embryos were manually dechorionated prior to transplantation. Fifty to 100 cells were transplanted into recipient *cmlc2*:GFP-uninjected embryos at the sphere to 30% epiboly stages by using capillary needles and adjusting balance pressure of PLI-100 microinjector (Harvard Apparatus, Holliston, MA) to move cells up and down the needle.

Overexpression and real-time RT-PCR analysis

Tg(*kdrl*:GFP) embryos were injected at the one- to two-cell stage with 55 pg of circular *etsrp*-XeX or human Ets1 plasmid DNA (Sumanas et al., 2008). Batches of 20 injected and control uninjected embryos were frozen on dry ice at the 10- and 20-somite stages. Total RNA was purified using the RNAquous-4PCR kit (Ambion). cDNA was synthesized using Superscript III Reverse Transcriptase and oligo-dT primer (Invitrogen). Real-time PCR was performed using Chromo4 thermal cycler (Bio-Rad) and iQ SYBR Green Supermix (Bio-Rad). The following PCR profile was used: 95°C for 5 minutes; 95°C for 1 minute, 58°C for 1 minute, 72°C for 1 minute, detection at 82°C for 10 seconds; steps 2-5 repeated 44 times. Relative cDNA amounts for most myocardial markers and *nfatc1* were calculated using the iCycler software (Bio-Rad) and normalized to the expression of *elongation factor 1a* (*ef1a*). As PCR amplification of *cmlc2* resulted in minor amounts of nonspecific products, the relative amount of specific *cmlc2* PCR product was calculated using ImageJ software (NIH) from the intensity values of an image of an ethidium bromide-stained agarose gel. Primer sequences are shown in Table S1 in the supplementary material.

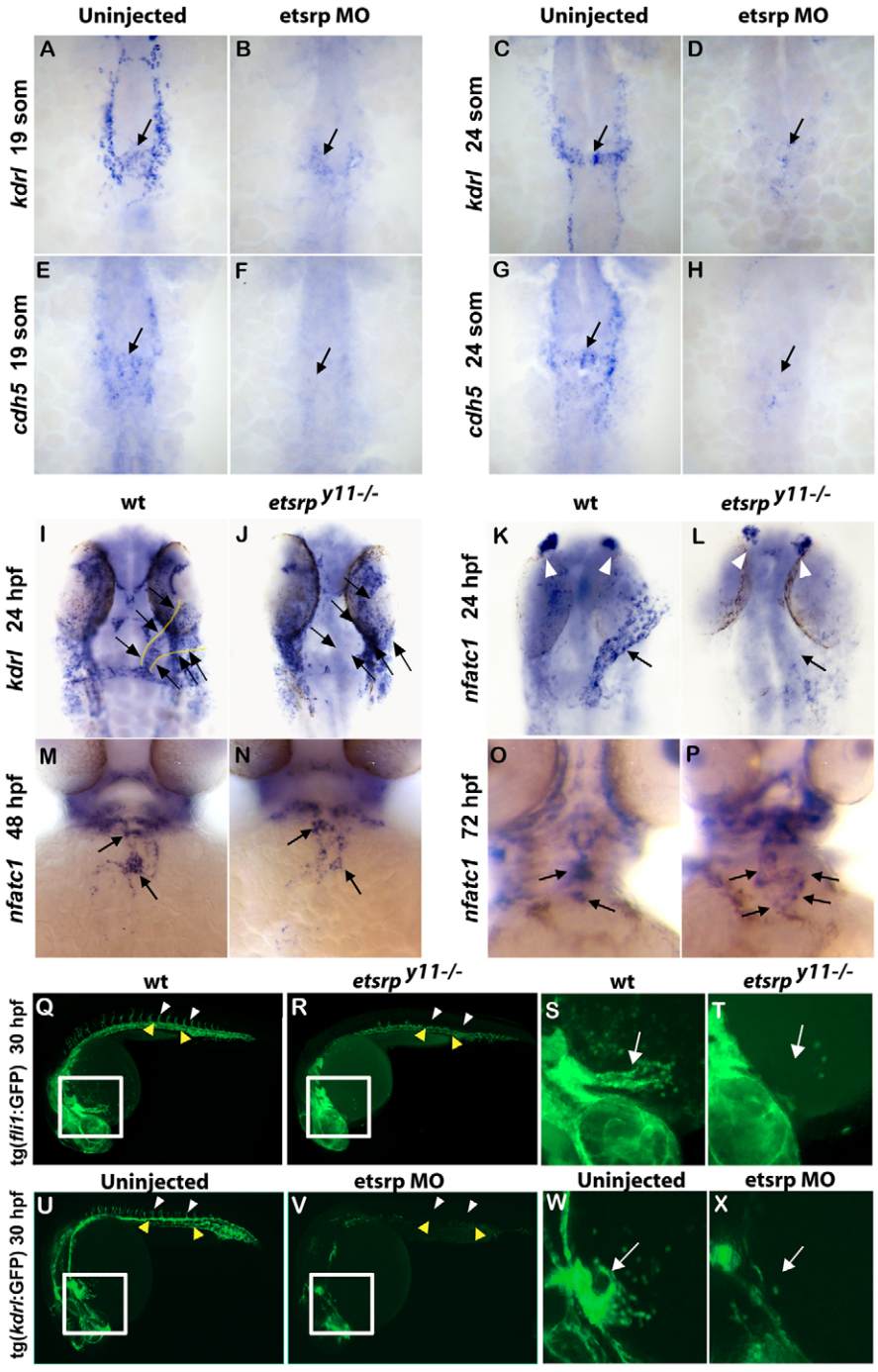

Fig. 1. Etsrp function is required for endocardium formation. (**A-H**) Morpholino knockdown of Etsrp results in the loss of early endocardial precursors (arrows) that migrate to the midline, as analyzed by in situ hybridization for endothelial/endocardial markers *kdrl* (A-D) and *cdh5* (E-H) at the 19-somite (A,B,E,F) and 24-somite (C,D,G,H) stages. (**I-L**) *etsrp*$^{y11-/-}$ mutants lack *kdrl* (I,J) and *nfatc1* (K,L) expression within the endocardial tube (arrows) at 24 hpf. Normal *kdrl* expression within the endocardium is outlined in yellow (I). *nfatc1* expression in olfactory placodes is not affected (white arrowheads). (**M-P**) At 48 hpf (M,N) and 72 hpf (O,P) stages, *nfatc1* expression in wild-type sibling embryos (M,O) is concentrated at the atrial/ventricular boundary (lower arrows) and the ventricular/outflow track boundary (upper arrows), but is sparse and diffuse in *etsrp*$^{y11-/-}$ mutants (N,P). (A-L) Ventral flat-mount view, anterior is upwards; (M-P) Ventral whole-mount view. (**Q-X**) Tg(*fli1*:GFP) (Q-T) and Tg(*kdrl*:GFP) (U-X) lines reveal loss of endocardial GFP in *etsrp*$^{y11-/-}$ mutants (R,T) and Etsrp morphants (V,X) at 30 hpf (insets in Q,R,U,V are shown a higher magnification in S,T,W,X, respectively). As expected, loss of Etsrp function results in the absence of intersegmental vessels (white arrowheads) and downregulation of *kdrl*:GFP and *fli1*:GFP in the axial vessels (yellow arrowheads). Lateral whole-mount view, anterior is towards the left. Arrows indicate endocardial tube.

Image capture and processing

Stained embryos were imaged by either whole mounting on glass slides in 2% methylcellulose or dehydrating in ethanol and whole mounting in araldite. Alternatively, flat mounting of stained or fixed transgenic embryos was carried out by either manually deyolking and mounting in 50% glycerol or dehydrating in ethanol and flat mounting in araldite. Images were captured with Sony DSC-H9 digital camera mounted on a Zeiss SV8 microscope or on an AxioImager Z1 (Zeiss) compound microscope with Axiocam color camera or monochrome cameras (Zeiss). Images in different focal planes were combined using the Extended Focus module within Axiovision software (Zeiss). Image levels were adjusted using Adobe Photoshop CS2 to increase the contrast.

Cell counting

Etsrp:GFP-expressing cells in ventrally mounted flattened embryos were counted using Bitplane Imaris, Autoquant and ImageJ software packages. Briefly, acquired *z*-stack images were cropped using the advanced cropping feature in Autoquant software to select those cells that had migrated to the midline. Cropped images were attenuation corrected and 3D deconvolved to remove out of focus fluorescence. Deconvolved *z*-stacks were exported as tiff files and imported into ImageJ or Imaris for cell counting. Tiff stacks were then maximum intensity projected using Imaris and exported to ImageJ for cell counting using pickpointer or counted in Imaris using the cell detection algorithm.

Electrophoretic mobility shift assay (EMSA)

DNA-binding reactions were performed as described previously (Dodou et al., 2003). Briefly, double-stranded oligonucleotides corresponding to the Mef2c-F10 ETS site (De Val et al., 2008) or the zebrafish *nfatc1* ETS site were labeled with [32P]-dCTP, using Klenow to fill in overhanging 5′ ends. Labeled probes were purified on a nondenaturing polyacrylamide-TBE gel. Binding reactions were incubated in 1× binding buffer [40 mM KCl, 15 mM HEPES (pH 7.9), 1 mM EDTA, 0.5 mM DTT, 5% glycerol] containing recombinant protein, 1.5 μg of poly-dI:dC and competitor DNA at room temperature for 10 minutes prior to probe addition. Reactions were incubated for an additional 20 minutes at room temperature after probe addition. Complexes were resolved by gel electrophoresis on a 6% nondenaturing polyacrylamide gel. The sense strand sequence of the zebrafish *nfatc1* ETS site used for EMSA is 5′-GGCAACAGCCTT-ACACAACAGGAAAC-3′. The sense strand sequence of the mutant *nfatc1* ETS site is 5′-GGCAACAGCCTTACACATCTAGAAAC-3′. Mouse Etv2 protein was synthesized using the TNT Coupled Transcription-Translation System (Promega). Plasmid pCS2-Etv2, used for in vitro synthesis of Etv2, has been described previously (De Val et al., 2008).

RESULTS

Etsrp function is required for endocardial differentiation

To determine whether Etsrp function is required for endocardial development, we analyzed Etsrp morpholino (MO) knockdown embryos (morphants) and *etsrp*^{y11}-null mutant embryos for endothelial and endocardial marker expression by in situ hybridization. Although endocardial precursors and vascular endothelial cells share expression of multiple genes, endocardial precursors can be distinguished from vascular endothelial cells after the 14-somite stage as they migrate to the midline to form the endocardial plate and the heart tube. At the 19- and 24-somite stages, uninjected embryos express *kdrl* (Fig. 1A,C) and *cdh5* (Fig. 1E,G) in vascular endothelial cells, located bilaterally, and in the endocardial cells at the midline. MO knockdown of Etsrp resulted

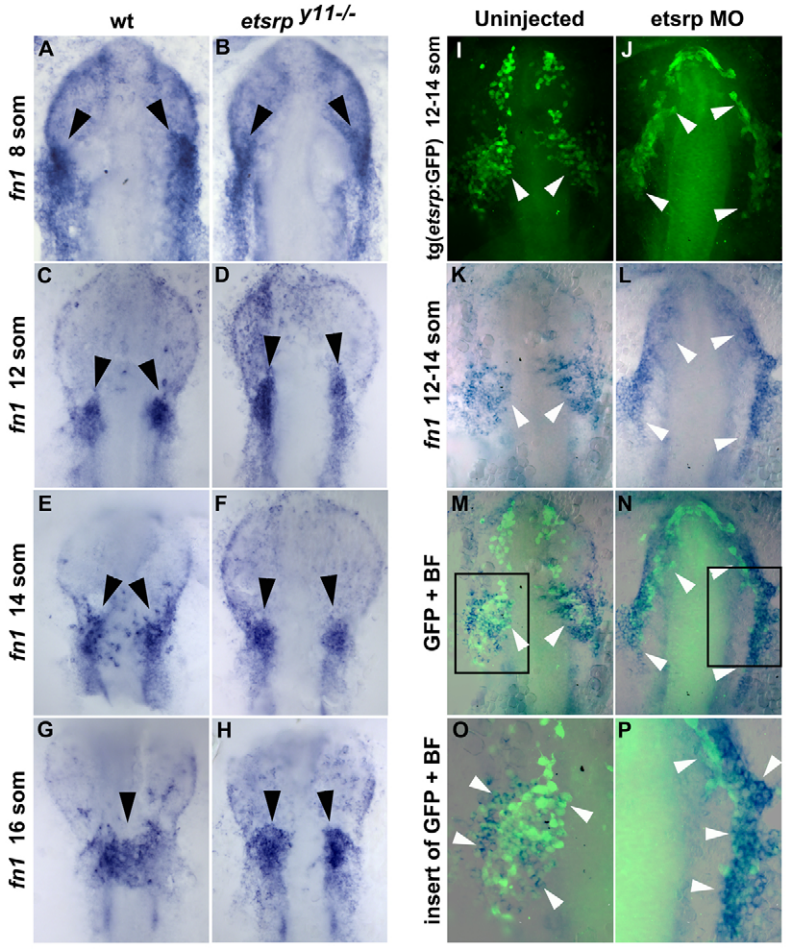

Fig. 2. Loss of Etsrp function results in the failure of *fibronectin 1*-expressing endocardial precursors to migrate towards the midline. (**A-D**) Fibronectin 1 (*fn1*) expression (arrowheads) in the presumptive endocardial precursors is slightly expanded rostrally in *etsrp*$^{y11-/-}$ mutants at the 8- to 12-somite stages, as analyzed by in situ hybridization. (**E-H**) *fn1*-expressing endocardial precursors (arrowheads) migrate to the midline in wild-type sibling embryos, while they remain localized bilaterally in *etsrp*$^{y11-/-}$ mutants at the 14- to 16-somite stages. (**I-P**) *fn1* expression largely overlaps with *etsrp*:GFP expression in the presumptive endocardial precursor cells (white arrowheads) in uninjected control embryos and *etsrp* morphants. Maximum projection image of *etsrp*:GFP immunofluorescence (I,J) and *fn1* in situ hybridization staining (K,L). Merged images of bright-field (BF) and GFP channels (M-P). There is slight expansion of *fn1* and *etsrp*:GFP staining in *etsrp* morphants. O,P are higher magnification views of the insets in M,N, respectively. (A-P) Ventral views of flat-mounted embryos, anterior is upwards.

in the loss vascular endothelial and endocardial staining for both *kdrl* (Fig. 1B,D) and *cdh5* (Fig. 1F,H). Similar absence or strong reduction in endocardial *kdrl* expression was observed in both *etsrp* morphants and *etsrp*^{y11} mutant embryos at 24 hpf, when the heart has formed a linear heart tube (Fig. 1I,J; data not shown).

We recently isolated the zebrafish *nfatc1* homolog, which is expressed specifically in endocardial but not vascular endothelial cells starting from 21 hpf and can be used as a marker for endocardial differentiation (K. S. Wong, K. Proulx, S. Palencia-Desai, V. Kohli, W. Hunter, J. D. Uhl and S. Sumanas, unpublished). In *etsrp*$^{y11-/-}$ embryos, *nfatc1* endocardial expression is completely missing at 24 hpf (Fig. 1K,L). By 48 hpf and 72 hpf, *etsrp*$^{y11-/-}$ embryos exhibit partial recovery of *nfatc1* expression, which remains reduced and diffuse throughout the endocardium (Fig. 1M-P).

Similar reduction or absence of GFP-expressing endocardial cells was observed in etsrp$^{y11-/-}$; *fli1*:GFP and *etsrp* MO-injected *kdrl*:GFP embryos at 30 hpf (Fig. 1Q-X). As expected, both lines exhibited severe reduction in endothelial GFP expression in trunk and tail region upon inhibition of *etsrp* function. Notably, *etsrp*$^{y11-/-}$; *fli1*:GFP transgenic embryos exhibited variable penetrance in endocardial reduction despite fairly uniform endothelial defects, as determined by the absence of intersegmental vessels. Seventy-nine percent of mutant embryos (22 out of 28) had very few remaining GFP+ endocardial cells, forming only small rudimentary tubes that failed to extend (Fig. 1T). The remaining 21% (six out of 28) of 30 hpf *etsrp*$^{y11-/-}$ mutants exhibited significant but less severe reduction in length and width of the endocardium (see Fig. S1 in the supplementary material). Altogether, these results argue that *etsrp* function is required for early endocardial differentiation.

Fn1-expressing endocardial progenitors fail to migrate towards the midline in the absence of Etsrp function

Fibronectin is thought to be one of the earliest markers for endocardial progenitors. In *cloche* mutants which are deficient in hematopoietic and vascular endothelial/endocardial lineages, *fn1* midline expression, which presumably corresponds to the endocardial progenitors, is absent (Trinh and Stainier, 2004). To gain further insight into how *etsrp* may affect endocardial development, we analyzed the expression of *fn1* at the 8- to 16-somite stages in wild-type and *etsrp*^{y11} mutant, as well as in MO knockdown embryos. Although *fn1* exhibits a complex expression pattern and is expressed in multiple cell types, the major group of anterior *fn1*-expressing cells at the 8- to 16-somite stages can be found in the ALPM, in the region corresponding to the midbrain organizing center (MOC) (Proulx et al., 2010), which gives rise to the majority of the cranial vessels, as well as to the myeloid and endocardial lineages (Fig. 2A,C). This *fn1* expression domain partially overlaps with *etsrp* expression (Fig. 2I,K,M,O) and is likely to include endocardial progenitors. In *y11*$^{-/-}$ mutant and *etsrp* morphant embryos at the 8- to 14-somite stages, *fn1* expression in the ALPM is mostly normal except for a slight expansion, mostly apparent at the 12-somite stage (Fig. 2A-D,I-P). At the 14- to 16-somite stages, the bilateral groups of *fn1*-expressing cells migrate

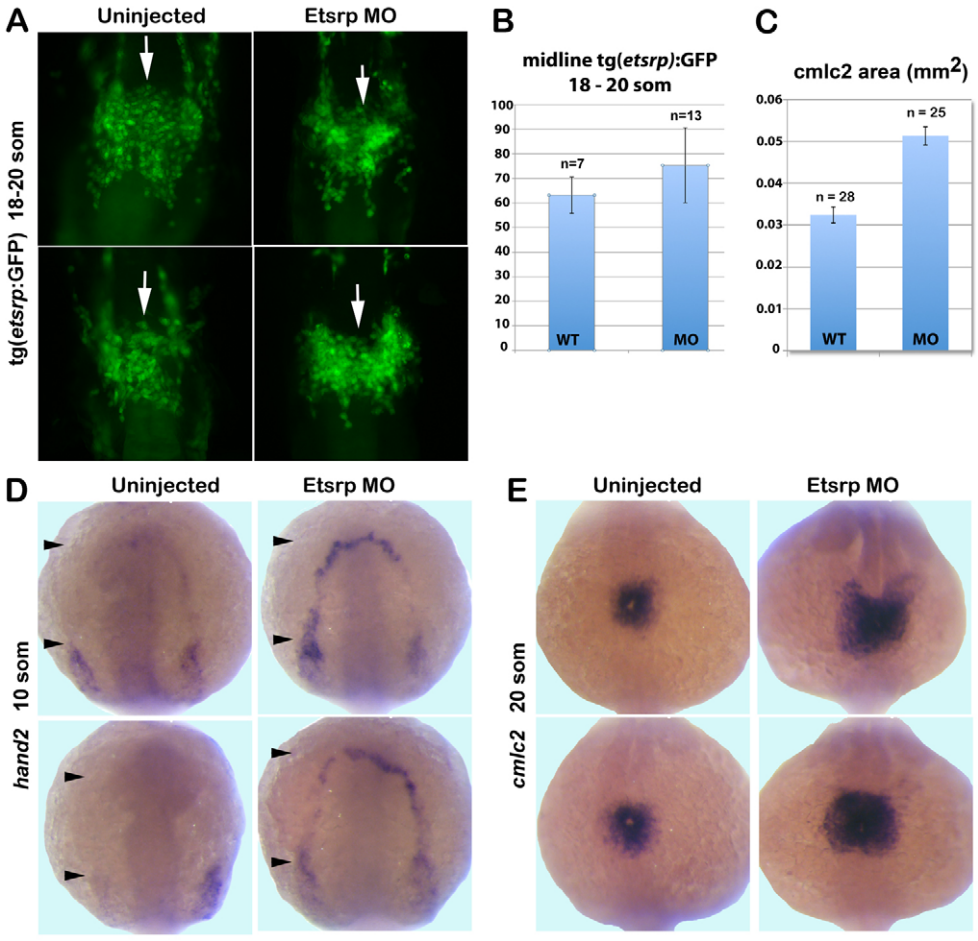

Fig. 3. Migration of *etsrp*:GFP-expressing cells is not affected while myocardial markers are expanded in *etsrp* morphants. (**A**) *etsrp*:GFP expression in the midline population (white arrows) of presumptive endocardial progenitors is not affected in Etsrp morphants (right panels) at the 18- to 20-somite stages. Maximum intensity projection of fixed Tg(*etsrp*:GFP) embryos, ventral flat-mounted view, anterior is upwards. (**B**) At the 18- to 20-somite stages, the relative numbers of *etsrp*:GFP+ putative cardiac progenitors that migrate to the midline are similar between uninjected controls and *etsrp* morphants. Data are mean±s.e.m. (**C**) The calculated average area (mm^2) of *cmlc2* in situ hybridization staining at the 20-somite stage shows a 58% increase in *etsrp* morphants compared with uninjected wild-type controls depicted in E. (**D**) *hand2* expression extends into the rostral ALPM (black arrowheads) in *etsrp* morphants but is absent from this region in the uninjected controls at the 10-somite stage. (**E**) *cmlc2* expression at 20-somite stage reveals radial expansion of the cardiac plate in *etsrp* morphants (right panels) compared with uninjected wild-type embryos (left panels). Anterodorsal whole-mount view, anterior is upwards.

towards the midline in wild-type embryos (Fig. 2E,G). In *etsrp* mutants, *fn1* expression remains bilateral, and *fn1*-expressing endocardial cells are absent from the midline, similar to the *clo* mutant phenotype (Fig. 2F,H).

To confirm the identity of *fn1*-expressing cells in wild-type and *etsrp* knockdown embryos, we used a *etsrp*:GFP reporter line to analyze *fn1* and *etsrp*:GFP co-expression using a combination of in situ hybridization and immunostaining against GFP. At the 12- to 14-somite stages, *etsrp* and *fn1* expression partially overlaps in wild-type embryos in the MOC region (Fig. 2I,K,M,O), where endocardial cells first emerge, as we have previously demonstrated by the time-lapse imaging of *etsrp*:GFP transgenic embryos (Proulx et al., 2010). We have previously shown that *etsrp* expression in the ALPM region is expanded in *etsrp* morphants (Sumanas et al., 2008), which suggests that additional cells within the ALPM are recruited to express *etsrp* in an attempt to initiate vascular development. Similar to *etsrp* expansion, *fn1* expression is also slightly expanded and closely overlaps with *etsrp* expression in *etsrp* morphants (Fig. 2J,L,N,P). These data suggest that $fn1^{+}etsrp^{+}$ double-positive cells include endocardial progenitors.

Myocardium is expanded in the absence of Etsrp function

In contrast to the absence of endocardial marker expression at the midline in *etsrp* morphants, our previous studies have argued that the migration of presumptive *etsrp*:GFP-positive endocardial progenitors to the midline is not affected in *etsrp* morphants (Proulx et al., 2010). Indeed, in *etsrp* morphants a population of *etsrp*:GFP cells is present at the midline in the region that normally corresponds to the endocardial precursors (Fig. 3A). Furthermore, the number of *etsrp*:GFP progenitor cells present at the midline is similar in wild-type embryos and *etsrp* morphants (Fig. 3B). Because these cells do not express endocardial markers, we hypothesized that at least some of them may have switched their fates and no longer represent endocardial progenitors.

Earlier studies have shown that inhibition of hematovascular development results in the rostral expansion of myocardial marker expression (Schoenebeck et al., 2007). Thus, expanded *hand2* expression has been observed in the *clo* mutant embryos and upon simultaneous inhibition of *etsrp* and *scl* function. Because our earlier studies showed that *etsrp* function is required for *scl* expression in the ALPM (Sumanas et al., 2008) we hypothesized that inhibition of *etsrp* function alone should be sufficient for the expansion of myocardial markers. Indeed, knockdown of Etsrp results in the rostral expansion of *hand2* expression (Fig. 3D). Furthermore, myocardial *cmlc2* expression is significantly expanded in Etsrp morphants (Fig. 3C,E).

Etsrp-expressing cells develop as cardiomyocytes in the absence of Etsrp function

These data demonstrate that *etsrp* morphants display simultaneous loss of endothelial and endocardial, and expansion of myocardial, lineages. Although the expansion of myocardial lineage has been previously observed in the absence of hematovascular development (Schoenebeck et al., 2007), the origin of these ectopic myocardial progenitors has not been established. We hypothesized that, in wild-type embryos, *etsrp* inhibits myocardial development in endothelial and endocardial progenitors, which develop as cardiomyocytes in the absence of *etsrp* function. To determine whether *etsrp*-expressing cells may initiate myocardial marker expression in the absence of *etsrp* function, we performed two-color in situ hybridization for *etsrp* and *hand2* expression at the 10-somite stage in wild-type and *etsrp* morphant embryos. In wild-type embryos, *etsrp* is expressed bilaterally along the ALPM just anterior to *hand2* expression (Fig. 4A) with no overlap. In Etsrp morphants, *hand2* expression extends rostrally where it overlaps with *etsrp* expression (Fig. 4B). This argues that *etsrp*-expressing cells initiate myocardial development in the absence of *etsrp* function.

To confirm whether some cardiomyocytes in *etsrp* morphants may be derived from *etsrp*-positive cells, we analyzed GFP and mCherry colocalization in double transgenic *etsrp*:GFP; *cmlc2*:mCherry embryos at 30 hpf. In wild-type embryos, *etsrp*:GFP expression is restricted to the endocardium, whereas *cmlc2*:mCherry expression is restricted to the myocardial layer and no overlap between the two transgenes is observed (0 out of 7 embryos analyzed, Fig. 4C). In *etsrp* morphants, *etsrp*:GFP expression can be observed in both endocardial and myocardial layers, where it overlaps with *cmlc2*:mCherry (16 out of 33 embryos analyzed contained $etsrp^{+}cmlc2^{+}$ cells; Fig. 4C). GFP/mCherry double-labeled cells were always in the myocardial

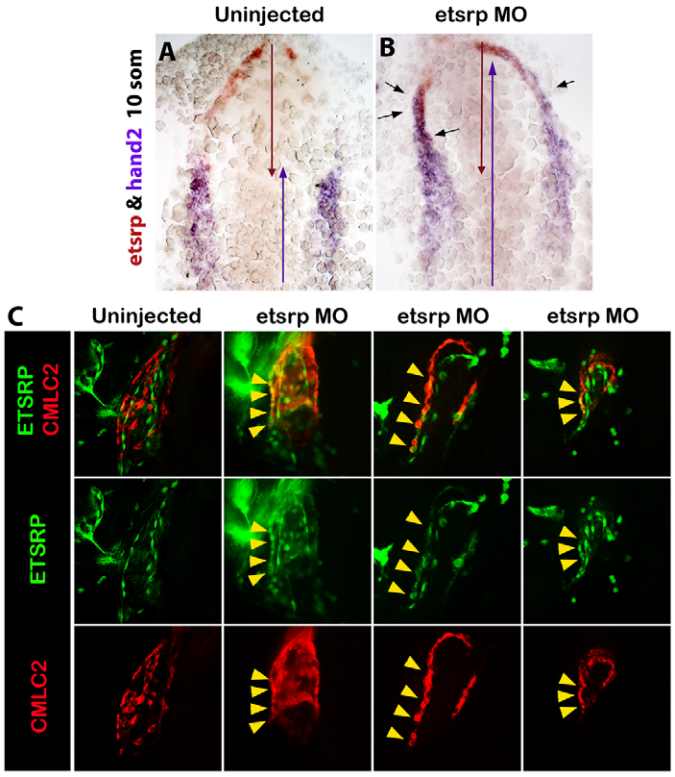

Fig. 4. *etsrp*-expressing cells differentiate as cardiomyocytes in the absence of Etsrp function. (**A**,**B**) Rostrally expanded *hand2* (purple) overlaps with *etsrp* (red) expression in Etsrp morphants (B) but not in wild-type embryos (A) at the 10-somite stage, as analyzed by two-color in situ hybridization. Red and purple arrows indicate the anterior-posterior span of *etsrp* and *hand2* expression, respectively. Black arrows indicate the areas of overlapping expression. Ventral flat-mounted view, anterior is upwards. (**C**) At 30 hpf, *etsrp*:GFP and *cmlc2*:mCherry expression overlaps (yellow arrowheads) in the myocardial layer of Etsrp morphant hearts (three right columns show three different morphants) but not in control uninjected embryos (left column). Left lateral whole-mount views of fixed Tg(*etsrp*:GFP; *cmlc2*:mCherry) embryos, anterior is towards the left. Projections of only few selected slices are shown.

layer, and randomly found throughout both the atrium and ventricle. Endocardial *etsrp*:GFP cells appear more sparse in *etsrp* morphants, consistent with the formation of reduced endocardium after 24 hpf. These data argue that in the absence of *etsrp* function, *etsrp*-expressing cells contribute to both endocardium and myocardium.

Etsrp overexpression results in the inhibition of endogenous myocardial markers and ectopic induction of both endocardial and myocardial marker expression

To determine whether *etsrp* overexpression is sufficient to inhibit myocardial and induce endocardial marker expression, we analyzed myocardial *hand2*, *cmlc2* and endocardial *nfatc1* expression in *etsrp*-overexpressing embryos by in situ hybridization and quantitative RT-PCR. As expected, microinjection of one-cell stage embryos with *etsrp* DNA overexpression construct resulted in a highly mosaic upregulation of *etsrp* and *kdrl*:GFP expression (data not shown). *Etsrp*-overexpressing embryos displayed variable reduction in myocardial *cmlc2* expression. In some cases, the entire left or right side of *cmlc2* expression within the cardiac plate was missing (Fig. 5A-D). In addition, embryos often displayed fusion defects of myocardial precursors. The phenotype was variable, probably owing to the highly mosaic nature of DNA overexpression. Unexpectedly, multiple *etsrp*-overexpressing embryos also displayed ectopic patches of *cmlc2*-expressing cells (Fig. 5A-D; see Table S2 in the supplementary material). Similarly, both patches of missing *hand2* expression and domains of ectopic *hand2*-expressing cells were present in *etsrp*-overexpressing embryos (Fig. 5E-L). As analyzed by qPCR, expression levels of myocardial *hand2*, *cmlc2*, *mef2a*, *mef2ca*, *tbx20* and endocardial *nfatc1* were significantly upregulated in *etsrp*-overexpressing embryos (Fig. 5M; see Table S3 in the supplementary material). However, *nkx2.5* and *vmhc* expression was not significantly affected (Fig. 5M; see Table S3 in the supplementary material). Overexpression of related human ETS1 caused no significant induction in *hand2*, *cmlc2* or *nfatc1* expression (see Table S4 in the supplementary material), demonstrating that the phenotype is specific to Etsrp overexpression.

Because the induction of ectopic myocardial marker expression by Etsrp was unexpected, we investigated this phenotype further. To determine whether Etsrp functions cell-autonomously to initiate myocardial development, cell transplantation was performed from Etsrp- and TRITC-dextran-injected *cmlc2*:GFP transgenic embryos into recipient uninjected *cmlc2*:GFP embryos. The embryos were subsequently analyzed at 24 hpf for the localization of *cmlc2*:GFP and TRITC fluorescence. The majority of ectopically located *cmlc2*:GFP cells did not display TRITC fluorescence, which argues that they did not originate from Etsrp-expressing cells (see Fig. S2A-C in the supplementary material). As analyzed by two-color in situ hybridization, ectopic *cmlc2*-positive cells frequently did not overlap with *etsrp* expression in Etsrp DNA-injected embryos (see Fig. S2D-I in the supplementary material). These results argue that Etsrp overexpression results in non-cell-autonomous induction of at least partial myocardial differentiation. However, because Etsrp during normal development is not expressed in myocardial progenitors and its function is not required for their differentiation, this phenotype is probably an artifact of Etsrp overexpression at high levels in different cell types where it is not normally expressed.

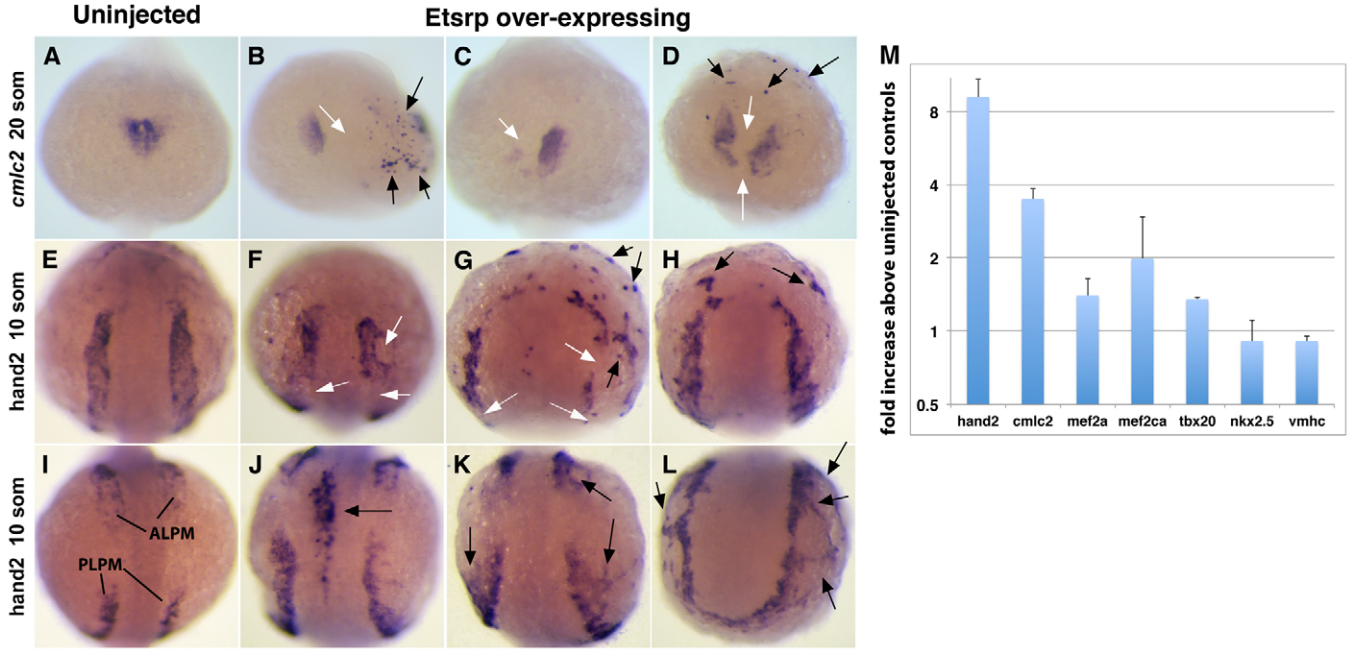

Fig. 5. Etsrp overexpression results in the loss of endogenous myocardial markers and the induction of ectopic myocardium. *cmlc2* (A-D) and *hand2* (E-L) expression analysis in uninjected (A,E,I) and *etsrp* DNA-injected (B-D,F-H,J-L) embryos. (**A-D**) Etsrp-overexpressing embryos exhibit fusion defects, missing cells (B-D, white arrows) and ectopic *cmlc2* expression at the 20-somite stage (B,D, black arrows). (**E-L**) At the 10-somite stage, Etsrp overexpression results in both disruption of endogenous *hand2* expression (F,G, white arrows) and induction of ectopic expression (black arrows, G,H,J-L). (A-H) Anterodorsal whole-mount view, anterior is upwards; (I-K) mid-dorsal view, anterior is upwards; (L) posterior view, dorsal is upwards. (**M**) Normalized ratio of myocardial marker expression in *etsrp* DNA-injected embryos versus wild-type embryos, as analyzed by qPCR. *y*-axis is shown in $[\log]_2$ scale. Data are mean±s.e.m.

Etv2 directly binds to Fox:Ets consensus sequence within the *nfatc1* promoter

Our results show that Etsrp function is both necessary and sufficient for early endocardial *nfatc1* expression. We then investigated whether Etsrp may directly regulate *nfatc1* expression. Recent evidence has demonstrated that a consensus Fox:Ets-binding motif bound by both Forkhead and Etsrp/Etv2 transcription factors is present in many endothelial specific enhancers and that binding of Etv2 and FoxC transcription factors synergistically induces endothelial specific gene expression (De Val et al., 2008). By analyzing *nfatc1* promoter regions of zebrafish and puffer fish *Tetraodon nigroviridis*, we identified a conserved region that contained consensus Ets and Fox:Ets-binding sites (Fig. 6A). As analyzed by EMSA assay, mouse Etv2 protein bound efficiently to the control and zebrafish *nfatc1* Ets sites (Fig. 6B, lanes 2,8). Binding to both sites was specifically competed by an excess of the wild-type, unlabeled control probe (Fig. 6B, lanes 3,9) but not by an equivalent amount of a mutant version of the control probe, which did not compete for binding to either probe (Fig. 6B, lanes 4,10). Unlabeled zebrafish *nfatc1* ETS probe also efficiently competed for binding to the control ETS site (lane 5) and to itself (lane 11). A mutant version of the *nfatc1* ETS probe in which the ETS consensus was disrupted did not compete for binding to either probe (Fig. 6B, lanes 6,12). These results argue that Etsrp/Etv2 directly binds to the *nfatc1* promoter.

Foxc1a is required and interacts with Etsrp in initiating endocardial differentiation but not inhibiting myocardial development

Previous studies have shown that *foxc1a* is required for zebrafish vascular development (De Val et al., 2008). To test whether *foxc1a* was required for the initiation of endocardial and inhibition of myocardial development, *foxc1a* morphants were analyzed for myocardial *hand2* and *cmlc2*, endocardial *nfatc1*, and *kdrl*:GFP expression. Knockdown of *foxc1a* using 1.5-4.0 ng *foxc1a* MO had no significant effect on myocardial *hand2* or *cmlc2* expression (Fig. 7A-H). A *foxc1a* MO injection (4 ng) resulted in apparent defects in somitogenesis (see Fig. S3 in the supplementary material), as reported previously (Topczewska et al., 2001). Doses of *foxc1a* MO above 4 ng resulted in high toxicity; therefore, we were not able to use higher MO doses for marker analysis. However, at the same doses, endocardial *nfatc1* and endocardial/endothelial *kdrl* expression were strongly reduced in *foxc1a* morphants (Fig. 7I-L; data not shown). In morphants injected with 1.5 ng of *foxc1a* MO, *nfatc1* expression is reduced, outlining a shorter thinner endocardium with fewer cells (Fig. 7J). Knockdown using 3 and 4 ng of *foxc1a* MO results in a severe reduction where most embryos have either no *nfatc1* staining at all or very few cells located in the ventricle region (Fig. 7K-M). Similarly, *kdrl*:GFP reporter embryos injected with *foxc1a* MO display strongly reduced endocardium (see Fig. S4 in the supplementary material). Similar results were also observed using a cocktail of two previously published *foxc1a*-specific MOs (see Fig. S5 in the supplementary material) (Topczewska et al., 2001). These results argue that *foxc1a* function is required for the endocardial development but is dispensable for the inhibition of myocardial formation.

As FoxC and Etsrp/Etv2 have been shown to act synergistically to promote endothelial gene transcription (De Val et al., 2008), we wanted to determine whether *foxc1a* and *etsrp* act synergistically in endocardial development. To test this interaction, we injected subphenotypic doses of *etsrp* MO and *foxc1a* MO individually or together. The endocardial tube formation is not significantly affected in *kdrl*:GFP transgenic embryos injected with a low dose of *etsrp* MO or a low dose of *foxc1a* MO (Fig. 8A-C). When both MOs are

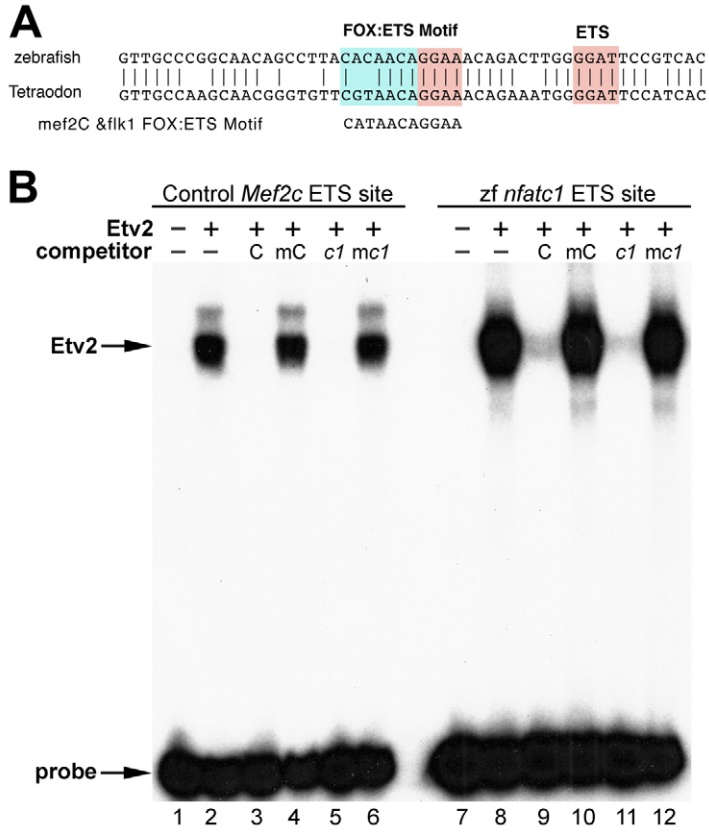

Fig. 6. Zebrafish Nfatc1 promoter contains a conserved ETS-binding site that interacts with Etv2 protein in vitro. (**A**) Zebrafish and puffer fish *Tetraodon nigroviridis* share a conserved sequence within Nfatc1 promoter region that contains a Fox:Ets consensus site that is also present in multiple endothelial enhancers such as *mef2c* and *flk1*. The conserved sequences are located –13.9 kb and –5.4 kb from the translation start sites of zebrafish and *Tetraodon* Nfatc1, respectively. Pink and blue regions indicate consensus ETS and FOX binding sites, respectively. (**B**) Etv2 binds to the zebrafish *nfatc1* site. Recombinant mouse Etv2 protein was used in EMSA with radiolabeled probes corresponding to a control ETS site from the mouse *Mef2c* gene (lanes 1-6) or to ETS site from the zebrafish *nfatc1* gene (lanes 7-12). Lanes 1 and 7 contain unprogramed rabbit reticulocyte lysate without recombinant Etv2 protein. Etv2 bound efficiently to the control and *nfatc1* ETS sites (lanes 2, 8). Binding to both sites was specifically competed by an excess of the wild-type unlabeled control (C) probe (lanes 3, 9) but not by an equivalent amount of a mutant version of the control probe (mC), which did not compete for binding to either probe (lanes 4, 10). Unlabeled zebrafish *nfatc1* ETS probe (c1) also efficiently competed for binding to the control ETS site (lane 5) and to itself (lane 11). A mutant version of the nfatc1 ETS probe in which the ETS consensus was disrupted (mc1) did not compete for binding to either probe (lanes 6, 12). A plus sign indicates addition of lysate containing recombinant Etv2. A minus sign indicates lysate without recombinant Etv2 in the top row and indicates no addition of ETS site competitor in the lower row.

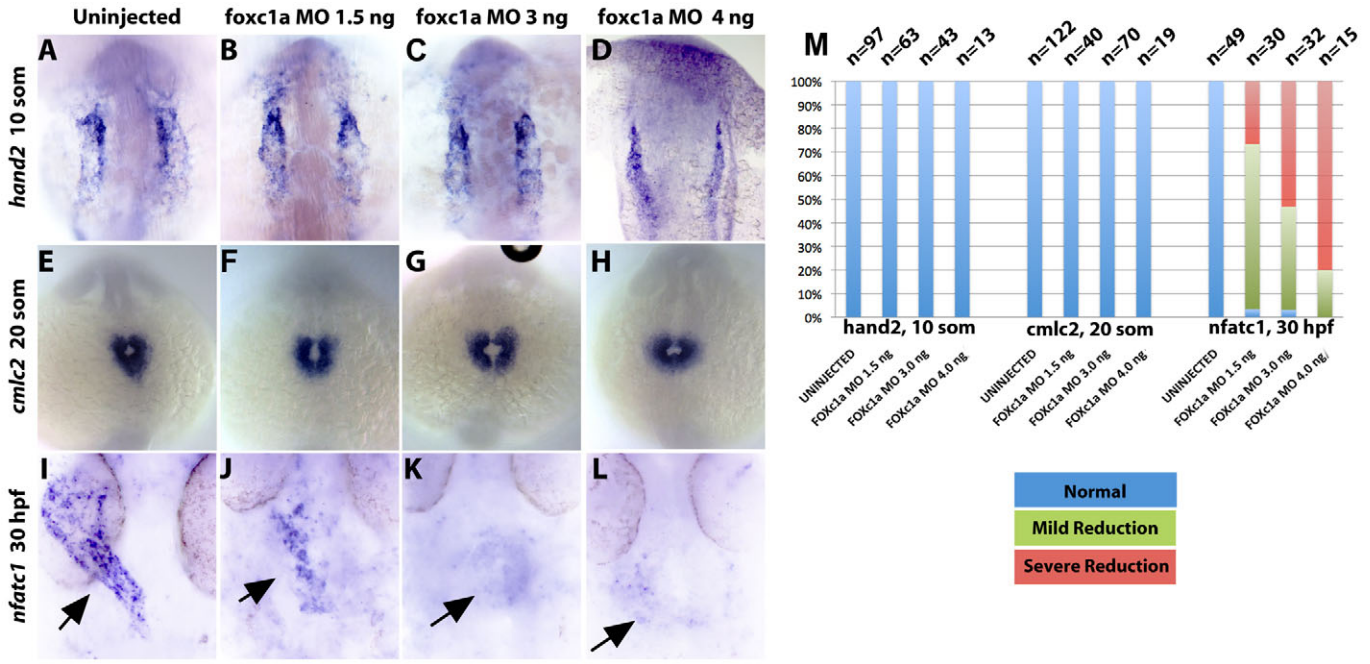

Fig. 7. *foxc1a* function is required for the initiation of endocardial development but not for inhibition of myocardial development. (**A-H**) *hand2* (A-D) and *cmlc2* (E-H) expression is not affected in Foxc1a morphant embryos, as analyzed by in situ hybridization at the 10-somite (A-D) and 20-somite (E-H) stages. (**I-L**) *nfatc1* expression (arrows) is reduced moderately at low *foxc1a* MO doses of 1.5 ng (J) and severely at higher doses of 3 ng and 4 ng (K,L) as detected by in situ hybridization. (A-L) Flat-mounted ventral views, anterior is upwards. (**M**) The severity and number of morphant embryos exhibiting endocardial reduction of *nfatc1* increases with the dose of *foxc1a* morpholino, while myocardial *hand2* and *cmlc2* expression is not affected significantly.

co-injected, the endocardium is severely reduced (Fig. 8D). This is also true for endocardial expression of *kdrl* at the 20-somite stage (Fig. 8E-H) and of *nfatc1* (Fig. 8I-L) at 30 hpf. By contrast, expression of myocardial markers *hand2* and *cmlc2* was not affected in *etsrp*, *foxc1a* and double *etsrp/foxc1a* morphants using the same MO doses (Fig. 8M-U). These results argue that *etsrp* and *foxc1a* interact during endocardial differentiation, whereas *etsrp* inhibits myocardial development in *foxc1a*-independent manner.

DISCUSSION

In this study, we show that a key regulator of vascular endothelial differentiation, Etsrp/Etv2, is also a crucial factor in endocardial-endothelial-myocardial lineage decisions. Our data show that Etsrp is required for endocardial differentiation by directly regulating *nfatc1* expression. At the same time, Etsrp function is required to inhibit myocardial differentiation. In the absence of Etsrp function, *etsrp*-expressing endothelial/endocardial progenitors differentiate as cardiomyocytes. Furthermore, Foxc1a function and Foxc1a/Etsrp interaction is required to initiate endocardial development but is dispensable for the inhibition of myocardial differentiation. This suggests that Etsrp initiates endothelial and endocardial and inhibits myocardial differentiation by two distinct mechanisms (Fig. 9).

It is currently not known whether myocardial, endocardial and endothelial lineages are derived from the same progenitor cells in zebrafish embryos. Earlier fate-mapping studies have argued that myocardial and endocardial lineages come from different spatial regions and are already separated during early gastrulation stages (Lee et al., 1994; Keegan et al., 2004). Our results support early separation of early endothelial/endocardial and myocardial progenitors. During normal development, *etsrp*:GFP expression is observed only in endothelial and endocardial but not myocardial progenitors (Proulx et al., 2010). Because GFP has a long half-life and its fluorescence can be observed for at least 24 hpf, even after its transcription has terminated, this argues that *etsrp* is never expressed in myocardial progenitors and the two lineages have already separated by the one-somite stage, when *etsrp* expression is first initiated within ALPM. However, because endocardial progenitors can differentiate as myocardial cells in the absence of *etsrp* function, this argues that endocardial cells retain developmental plasticity until much later stages and their fates can be reprogrammed.

Although previous studies have demonstrated myocardial expansion within the ALPM in the absence of hematovascular development (Schoenebeck et al., 2007), the origin of ectopic cardiomyocytes was not known. Our studies argue that endothelial-endocardial precursors cell-autonomously initiate myocardial differentiation in the absence of Etsrp function. It is possible that myocardial development is the 'default' fate within the ALPM in the absence of hematovascular development. However, our results show that in the absence of *foxc1a* function, endocardial differentiation is inhibited while myocardial differentiation is not affected. Furthermore, although co-injection of subphenotypic doses of *etsrp* MO and *foxc1a* MOs results in the absence of both endocardial and vascular endothelial marker expression within the ALPM, no increase in myocardial marker expression is observed. These results argue that inhibition of endothelial-endocardial development by itself is not sufficient to initiate myocardial development and high inhibition levels of Etsrp function are necessary. Furthermore, these results suggest that *etsrp* represses myocardial development in *foxc1a*-independent manner, perhaps by recruiting transcriptional repressors.

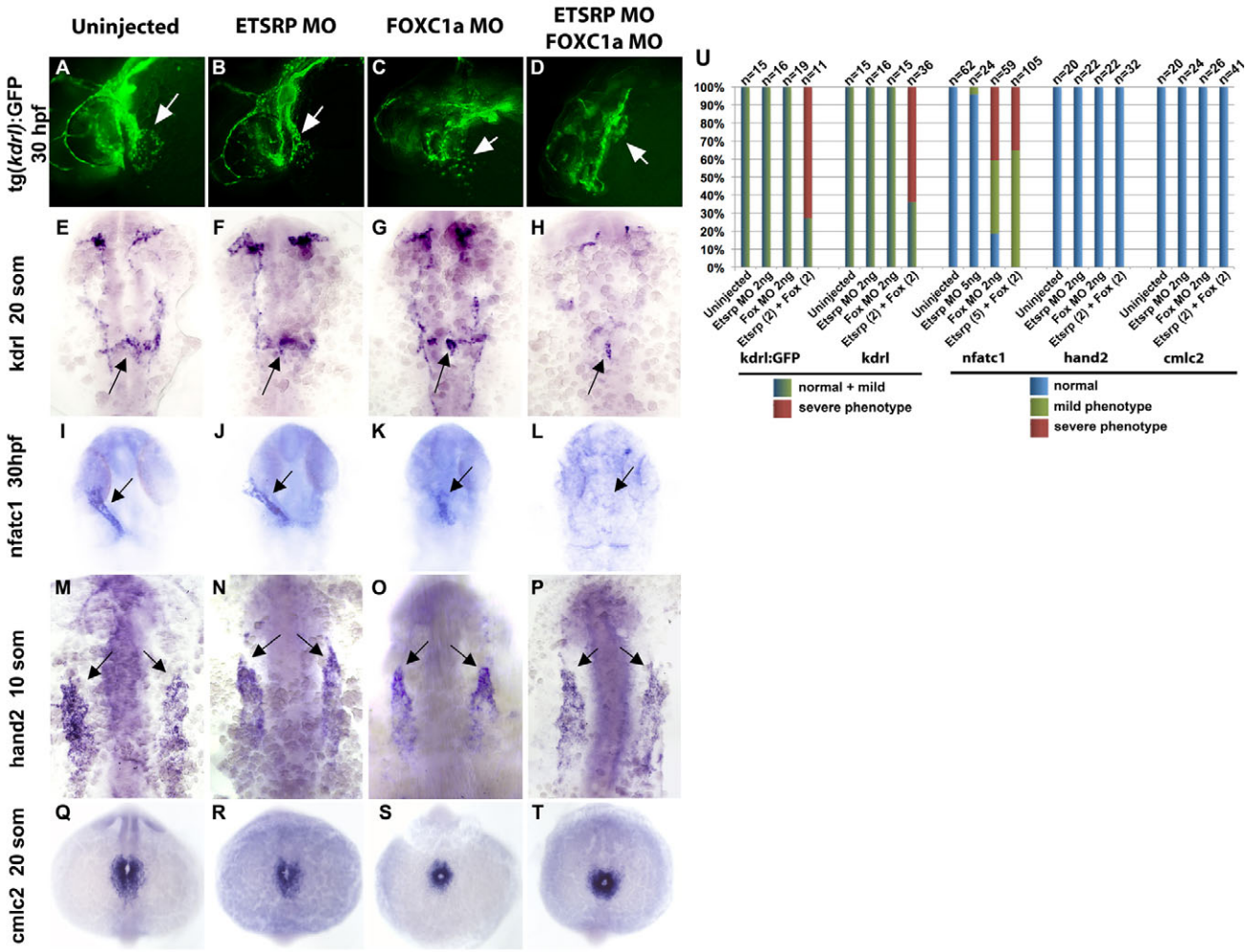

Fig. 8. Simultaneous Foxc1a and Etsrp knockdown affects endocardial but not myocardial development. (**A-L**) Endocardial markers *kdrl*:GFP at 30 hpf (A-D, arrows), *kdrl* at the 20-somite stage (E-H, arrows) and *nfatc1* at 30 hpf (I-L, arrows) show no or only a slight reduction in expression in embryos injected with low doses of either 2 ng Etsrp MO (B,F,J) or 2 ng Foxc1a MO (C,G,K) compared with uninjected controls (A,E,I). However, upon simultaneous knockdown of Etsrp and Foxc1a, levels of all of these endocardial markers are severely reduced (D,H,L). (**M-T**) Myocardial *hand2* expression at the 10-somite stage (M-P, arrows show anterior border) and *cmlc2* at the 20-somite stage (Q-T) are not significantly affected in 2 ng *etsrp* MO-injected (N,R), 2 ng Foxc1a MO-injected (O,S) or Etsrp/Foxc1a MO co-injected (P,T) embryos compared with uninjected controls (M,Q). (A-D) Whole-mount fluorescent images of fixed Tg(*kdrl*:GFP) embryos at 30 hpf, anterior is towards the left, dorsal is upwards. (E-P) Ventral flat-mount view of in situ hybridization analysis, anterior is upwards. (Q-T) Anterodorsal whole-mount view, anterior is upwards. (**U**) Phenotypic distribution of endocardial *kdrl*:GFP, *kdrl, nfatc1* and myocardial *hand2* expression in *etsrp, foxc1a* and *etsrp/foxc1a* MO-injected embryos. The blue bars represent no change, whereas the green and red bars indicate mild and severe reduction in endocardial expression, respectively. Note that for *kdrl*:GFP and *kdrl* expression, normal or mildly reduced categories are combined and shown in dark green because it was difficult to distinguish the two categories.

Previous studies have suggested that *fn1* expression within ALPM corresponds to early endocardial progenitors (Trinh and Stainier, 2004), which is consistent with our results. Early *fn1* expression only partially overlaps with *etsrp* expression, suggesting that not all *fn1*-expressing cells within ALPM are endocardial progenitors. In contrast to other endocardial markers, *fn1* expression in Etsrp mutants or morphants remains localized bilaterally, whereas a pool of *etsrp*:GFP-expressing cells migrate to the midline. These results argue that *etsrp* function is required for the midline migration of $fn1^{+}$ endocardial progenitors. Furthermore, it suggests that *etsrp*:GFP cells present at the midline in *etsrp* morphants include myocardial progenitors, and *etsrp* function is not required for their migration. In support of this hypothesis, at least some *etsrp*:GFP cells co-express *cmlc2* and thus differentiate as cardiomyocytes in *etsrp* morphants.

Etsrp overexpression has been known to result in the precocious and ectopic induction of multiple endothelial-specific genes. As our results show, it also results in strong precocious induction of endocardial *nfatc1* expression, as analyzed at the 20-somite stage. This argues that Etsrp is sufficient to induce both endothelial and endocardial differentiation. Based on EMSA analysis, Etsrp binds directly to the evolutionarily conserved *nfatc1* enhancer, which argues that Etsrp directly regulates *nfatc1* transcription. Unexpectedly, *etsrp* overexpression resulted in both inhibition of endogenous and induction of ectopic myocardial marker

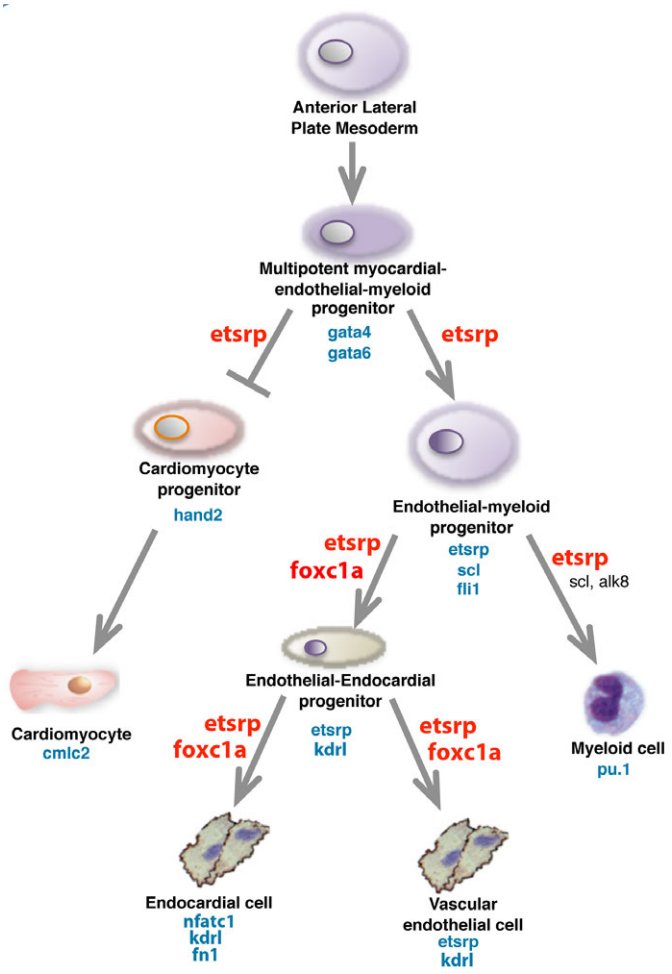

Fig. 9. A proposed model for specification of cardiovascular lineages within the zebrafish ALPM. Etsrp promotes vascular endothelial and endocardial differentiation by interacting with Foxc1a, whereas Etsrp function is required to inhibit myocardial differentiation in Foxc1a-independent manner. In the absence of Etsrp function, multipotent progenitors initiate myocardial differentiation.

expression. As demonstrated by cell transplantation analysis, ectopic myocardial marker induction is non-cell-autonomous. It is likely that overexpression of Etsrp results in an induction of a secreted signaling molecule that can promote myocardial development. However, because during normal development Etsrp is not expressed in myocardial progenitors and is not required for cardiomyogenesis, this Etsrp overexpression phenotype may be an artifact caused by high doses of Etsrp protein present in many different cell types.

In summary, this study establishes Etsrp as a crucial regulator of early cardiovascular development, and argues that Etsrp promotes endothelial and endocardial development and represses myocardial differentiation by two independent mechanisms. Mouse Etv2 mutants also display endothelial and endocardial defects (Lee et al., 2008; Ferdous et al., 2009), which suggests that the Etsrp/Etv2 mechanism of function is evolutionarily conserved. These results are important for our understanding of normal cardiovascular development in vertebrates and will greatly contribute to the stem cell research aimed at regenerating heart tissues, eventually leading to new strategies in treating heart disorders.

Acknowledgements
We thank B. Weinstein for sharing the y11 mutant zebrafish line.

Funding
This research was supported by the March of Dimes Basil O'Connor award [5-FY09-78 to S.S.], by the National Institutes of Health [HL64658 to B.L.B. and DP2OD007464-01 to N.C.C.] and by the Cincinnati Children's Research Foundation [to S.S.]. Deposited in PMC for release after 12 months.

Competing interests statement
The authors declare no competing financial interests.

Supplementary material
Supplementary material for this article is available at
http://dev.biologists.org/lookup/suppl/doi:10.1242/dev.064998/-/DC1

References

Brown, L. A., Rodaway, A. R., Schilling, T. F., Jowett, T., Ingham, P. W., Patient, R. K. and Sharrocks, A. D. (2000). Insights into early vasculogenesis revealed by expression of the ETS-domain transcription factor Fli-1 in wild-type and mutant zebrafish embryos. *Mech. Dev.* **90**, 237-252.
Bussmann, J., Bakkers, J. and Schulte-Merker, S. (2007). Early endocardial morphogenesis requires Scl/Tal1. *PLoS Genet.* **3**, e140.
de la Pompa, J. L., Timmerman, L. A., Takimoto, H., Yoshida, H., Elia, A. J., Samper, E., Potter, J., Wakeham, A., Marengere, L., Langille, B. L. et al. (1998). Role of the NF-ATc transcription factor in morphogenesis of cardiac valves and septum. *Nature* **392**, 182-186.
De Val, S., Chi, N. C., Meadows, S. M., Minovitsky, S., Anderson, J. P., Harris, I. S., Ehlers, M. L., Agarwal, P., Visel, A., Xu, S. M. et al. (2008). Combinatorial regulation of endothelial gene expression by ets and forkhead transcription factors. *Cell* **135**, 1053-1064.
Dodou, E., Xu, S. M. and Black, B. L. (2003). mef2c is activated directly by myogenic basic helix-loop-helix proteins during skeletal muscle development in vivo. *Mech. Dev.* **120**, 1021-1032.
Ferdous, A., Caprioli, A., Iacovino, M., Martin, C. M., Morris, J., Richardson, J. A., Latif, S., Hammer, R. E., Harvey, R. P., Olson, E. N. et al. (2009). Nkx2-5 transactivates the Ets-related protein 71 gene and specifies an endothelial/endocardial fate in the developing embryo. *Proc. Natl. Acad. Sci. USA* **106**, 814-819.
Harris, I. S. and Black, B. L. (2010). Development of the endocardium. *Pediatr. Cardiol.* **31**, 391-399.
Huang, C. J., Tu, C. T., Hsiao, C. D., Hsieh, F. J. and Tsai, H. J. (2003). Germ-line transmission of a myocardium-specific GFP transgene reveals critical regulatory elements in the cardiac myosin light chain 2 promoter of zebrafish. *Dev. Dyn.* **228**, 30-40.
Jin, S. W., Beis, D., Mitchell, T., Chen, J. N. and Stainier, D. Y. (2005). Cellular and molecular analyses of vascular tube and lumen formation in zebrafish. *Development* **132**, 5199-5209.
Jowett, T. (1999). Analysis of protein and gene expression. *Methods Cell Biol.* **59**, 63-85.
Kattman, S. J., Huber, T. L. and Keller, G. M. (2006). Multipotent flk-1+ cardiovascular progenitor cells give rise to the cardiomyocyte, endothelial, and vascular smooth muscle lineages. *Dev. Cell* **11**, 723-732.
Keegan, B. R., Meyer, D. and Yelon, D. (2004). Organization of cardiac chamber progenitors in the zebrafish blastula. *Development* **131**, 3081-3091.
Kimmel, C. B., Ballard, W. W., Kimmel, S. R., Ullmann, B. and Schilling, T. F. (1995). Stages of embryonic development of the zebrafish. *Dev. Dyn.* **203**, 253-310.
Larson, J. D., Wadman, S. A., Chen, E., Kerley, L., Clark, K. J., Eide, M., Lippert, S., Nasevicius, A., Ekker, S. C., Hackett, P. B. et al. (2004). Expression of VE-cadherin in zebrafish embryos: a new tool to evaluate vascular development. *Dev. Dyn.* **231**, 204-213.
Lawson, N. D. and Weinstein, B. M. (2002). In vivo imaging of embryonic vascular development using transgenic zebrafish. *Dev. Biol.* **248**, 307-318.
Lee, D., Park, C., Lee, H., Lugus, J. J., Kim, S. H., Arentson, E., Chung, Y. S., Gomez, G., Kyba, M., Lin, S. et al. (2008). ER71 acts downstream of BMP, Notch, and Wnt signaling in blood and vessel progenitor specification. *Cell Stem Cell* **2**, 497-507.
Lee, R. K., Stainier, D. Y., Weinstein, B. M. and Fishman, M. C. (1994). Cardiovascular development in the zebrafish. II. Endocardial progenitors are sequestered within the heart field. *Development* **120**, 3361-3366.
Liao, E. C., Paw, B. H., Oates, A. C., Pratt, S. J., Postlethwait, J. H. and Zon, L. I. (1998). SCL/Tal-1 transcription factor acts downstream of cloche to specify hematopoietic and vascular progenitors in zebrafish. *Genes Dev.* **12**, 621-626.
Liao, W., Bisgrove, B. W., Sawyer, H., Hug, B., Bell, B., Peters, K., Grunwald, D. J. and Stainier, D. Y. (1997). The zebrafish gene cloche acts upstream of a flk-1 homologue to regulate endothelial cell differentiation. *Development* **124**, 381-389.

Lough, J. and Sugi, Y. (2000). Endoderm and heart development. *Dev. Dyn.* **217**, 327-342.
Misfeldt, A. M., Boyle, S. C., Tompkins, K. L., Bautch, V. L., Labosky, P. A. and Baldwin, H. S. (2009). Endocardial cells are a distinct endothelial lineage derived from Flk1+ multipotent cardiovascular progenitors. *Dev. Biol.* **333**, 78-89.
Moretti, A., Caron, L., Nakano, A., Lam, J. T., Bernshausen, A., Chen, Y., Qyang, Y., Bu, L., Sasaki, M., Martin-Puig, S. et al. (2006). Multipotent embryonic isl1+ progenitor cells lead to cardiac, smooth muscle, and endothelial cell diversification. *Cell* **127**, 1151-1165.
Pham, V. N., Lawson, N. D., Mugford, J. W., Dye, L., Castranova, D., Lo, B. and Weinstein, B. M. (2007). Combinatorial function of ETS transcription factors in the developing vasculature. *Dev. Biol.* **303**, 772-783.
Proulx, K., Lu, A. and Sumanas, S. (2010). Cranial vasculature in zebrafish forms by angioblast cluster-derived angiogenesis. *Dev. Biol.* **348**, 34-46.
Robu, M. E., Larson, J. D., Nasevicius, A., Beiraghi, S., Brenner, C., Farber, S. A. and Ekker, S. C. (2007). p53 activation by knockdown technologies. *PLoS Genet.* **3**, e78.
Schoenebeck, J. J., Keegan, B. R. and Yelon, D. (2007). Vessel and blood specification override cardiac potential in anterior mesoderm. *Dev. Cell* **13**, 254-267.
Shaner, N. C., Campbell, R. E., Steinbach, P. A., Giepmans, B. N., Palmer, A. E. and Tsien, R. Y. (2004). Improved monomeric red, orange and yellow fluorescent proteins derived from Discosoma sp. red fluorescent protein. *Nat. Biotechnol.* **22**, 1567-1572.
Simoes, F. C., Peterkin, T. and Patient, R. (2011). Fgf differentially controls cross-antagonism between cardiac and haemangioblast regulators. *Development* **138**, 3235-3245.
Stainier, D. Y., Weinstein, B. M., Detrich, H. W., 3rd, Zon, L. I. and Fishman, M. C. (1995). Cloche, an early acting zebrafish gene, is required by both the endothelial and hematopoietic lineages. *Development* **121**, 3141-3150.
Sumanas, S. and Lin, S. (2006). Ets1-related protein is a key regulator of vasculogenesis in zebrafish. *PLoS Biol.* **4**, e10.
Sumanas, S., Zhang, B., Dai, R. and Lin, S. (2005). 15-zinc finger protein Bloody Fingers is required for zebrafish morphogenetic movements during neurulation. *Dev. Biol.* **283**, 85-96.
Sumanas, S., Gomez, G., Zhao, Y., Park, C., Choi, K. and Lin, S. (2008). Interplay among Etsrp/ER71, Scl, and Alk8 signaling controls endothelial and myeloid cell formation. *Blood* **111**, 4500-4510.
Thompson, M. A., Ransom, D. G., Pratt, S. J., MacLennan, H., Kieran, M. W., Detrich, H. W., 3rd, Vail, B., Huber, T. L., Paw, B., Brownlie, A. J. et al. (1998). The cloche and spadetail genes differentially affect hematopoiesis and vasculogenesis. *Dev. Biol.* **197**, 248-269.
Topczewska, J. M., Topczewski, J., Shostak, A., Kume, T., Solnica-Krezel, L. and Hogan, B. L. (2001). The winged helix transcription factor Foxc1a is essential for somitogenesis in zebrafish. *Genes Dev.* **15**, 2483-2493.
Trinh, L. A. and Stainier, D. Y. (2004). Fibronectin regulates epithelial organization during myocardial migration in zebrafish. *Dev. Cell* **6**, 371-382.
Wu, S. M., Fujiwara, Y., Cibulsky, S. M., Clapham, D. E., Lien, C. L., Schultheiss, T. M. and Orkin, S. H. (2006). Developmental origin of a bipotential myocardial and smooth muscle cell precursor in the mammalian heart. *Cell* **127**, 1137-1150.
Yang, L., Soonpaa, M. H., Adler, E. D., Roepke, T. K., Kattman, S. J., Kennedy, M., Henckaerts, E., Bonham, K., Abbott, G. W., Linden, R. M. et al. (2008). Human cardiovascular progenitor cells develop from a KDR+ embryonic-stem-cell-derived population. *Nature* **453**, 524-528.
Yelon, D., Horne, S. A. and Stainier, D. Y. (1999). Restricted expression of cardiac myosin genes reveals regulated aspects of heart tube assembly in zebrafish. *Dev. Biol.* **214**, 23-37.
Yelon, D., Ticho, B., Halpern, M. E., Ruvinsky, I., Ho, R. K., Silver, L. M. and Stainier, D. Y. (2000). The bHLH transcription factor hand2 plays parallel roles in zebrafish heart and pectoral fin development. *Development* **127**, 2573-2582.